Exciton annihilation and transport in fifth order electronic spectroscopy

C. Heshmatpour [1,2], J. Hauer [2, 3], F. Šanda [1]

1 Institute of Physics, Faculty of Mathematics and Physics, Charles University, Ke Karlovu 5, Prague 121 16, Czech Republic

2 Professur für Dynamische Spektroskopien, Fakultät für Chemie, Technische Universität München, Lichtenbergstr. 4, D- 85748, Garching b. München, Germany

3 Photonics Institute, TU Wien, Gußhausstraße 27-29, 1040 Vienna, Austria

Motivation

Multidimensional fifth order spectroscopy (R^5-2D-ES) is a sophisticated and specialized tool for probing bi-exciton dynamics [1,2]. Here, we present an analysis of fifth order signals emitted into $\pm 2\boldsymbol{K}_1 \mp 2\boldsymbol{K}_2 + \boldsymbol{K}_3$ phase matching directions. In an effort to model fifth order electronic spectra of tractably small systems, we develop a dynamical model for molecular dimers and trimers. **We show that fifth order two-dimensional spectroscopy allows to track and pinpoint population transfer- and annihilation dynamics of bi-excitons, without the need to perform and analyse intensity dependent experiments.**

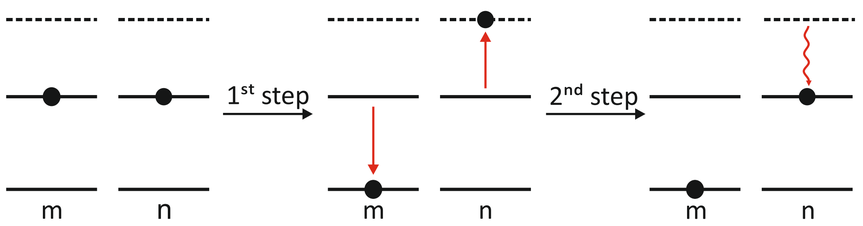

Fig. 1: Microscopic picture of EEA [3]: (1) excitation energy is resonantly transferred between two adjacent sites *m* and *n*. This transfer stimulates one site back to the ground state whereas the other is promoted to a higher lying state. (2) Phonon-assisted non-radiative relaxation back to the first excited state.

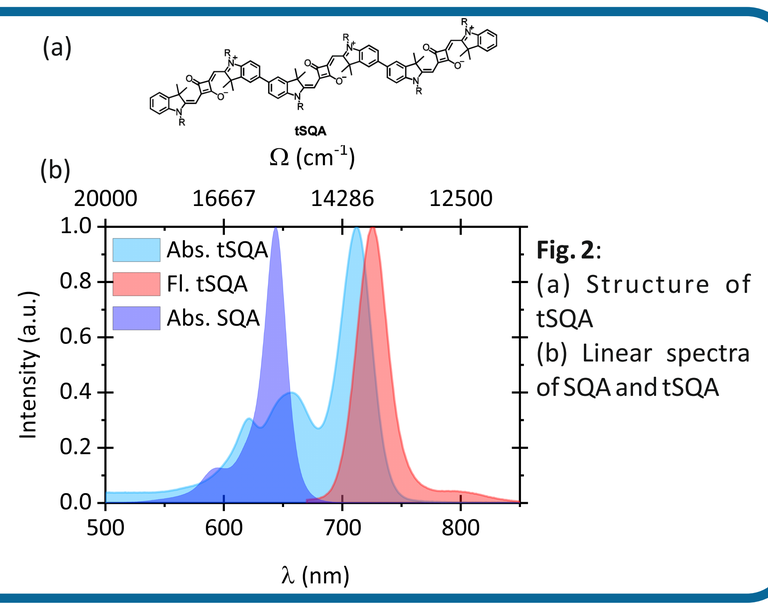

Fig. 2:
(a) Structure of tSQA
(b) Linear spectra of SQA and tSQA

Multidimensional line shapes of the fifth order response

Fifth order signals:

$$R^{(5)}_{NR}(t_1,t_2,t_3) = (i)^5 \langle\langle \mu | \breve{\mathcal{G}}(t_3)\breve{\mu}^{(+)}\breve{\mathcal{G}}(t_2)\breve{\mu}^{(-)}\breve{\mu}^{(-)}\breve{\mathcal{G}}(t_1)\breve{\mu}^{(+)}\breve{\mu}^{(+)}|gg\rangle\rangle$$

$$R^{(5)}_{R}(t_1,t_2,t_3) = (i)^5 \langle\langle \mu | \breve{\mathcal{G}}(t_3)\breve{\mu}^{(+)}\breve{\mathcal{G}}(t_2)\breve{\mu}^{(+)}\breve{\mu}^{(+)}\breve{\mathcal{G}}(t_1)\breve{\mu}^{(-)}\breve{\mu}^{(-)}|gg\rangle\rangle$$

Dipole superoperator actions:

$$\breve{\mu}^{(+)}\hat{X} = \sum_{n=1}^{N} d_n(\hat{B}_n^\dagger \hat{X} - \hat{X}\hat{B}_n^\dagger)$$

$$\breve{\mu}^{(-)}\hat{X} = \sum_{n=1}^{N} d_n(\hat{B}_n \hat{X} - \hat{X}\hat{B}_n)$$

d_n ... transition dipole moment of molecule *n*

$\hat{B}_n^\dagger(\hat{B}_n)$ ... creation (annihilation) operator of excitation at site *n*

Green's function:

$$\breve{\mathcal{G}}(t) = \exp\left(\left(\breve{\mathcal{D}} + \breve{\mathcal{A}}\right)t\right)$$

$\breve{\mathcal{D}}$ ... generator for transport: Redfield and Förster

$\breve{\mathcal{A}}$ ... generator for annihilation dynamics

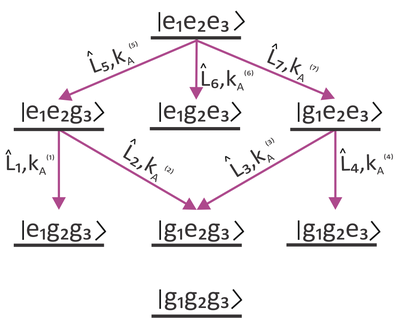

Fig. 3: EEA in a molecular trimer is modeled as unidirectional transport to lower excitonic manifolds induced by operators $\{L_i\}$ and rates $k_A^{(i)}$, as indicated by purple arrows.

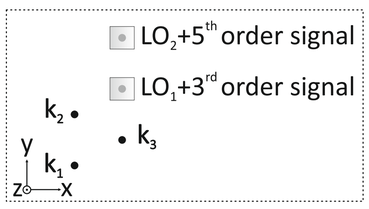

Fig. 4: Schematic of the experimental phase matching geometry

$2k_1$-$2k_2$+k_3:	GSB	ESA		SE		SE ESA
t_2 dynamics	/	Coherence l≠m	Transport m→n	Coherence i≠j	Transport l→m	Exciton Exciton Annihilation
bi-exciton dynamics	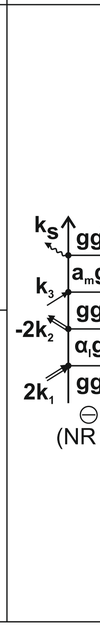 (NR 1)	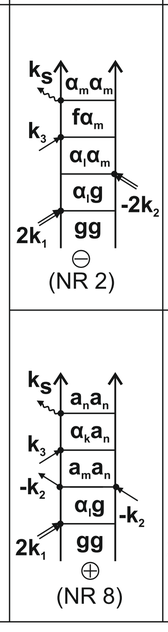 (NR 2)	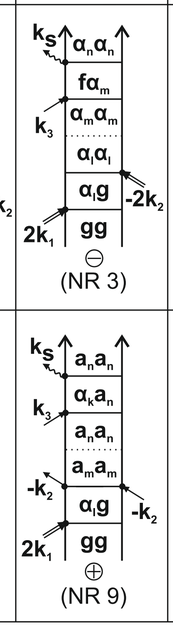 (NR 3)	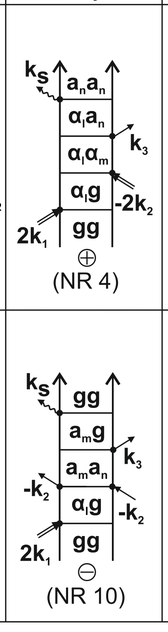 (NR 4)	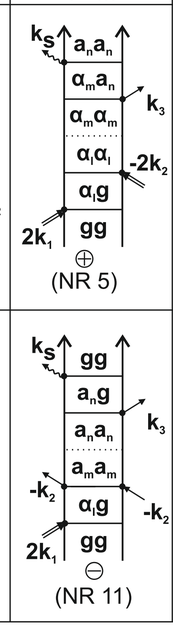 (NR 5)	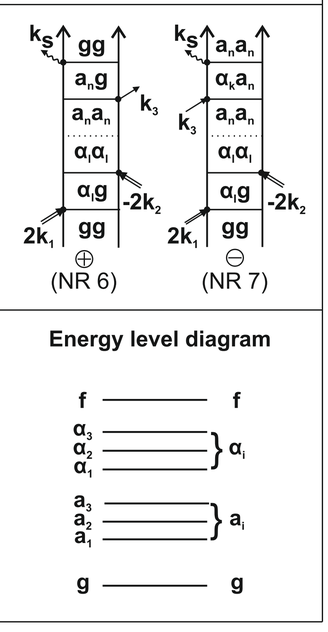 (NR 6) (NR 7)
single-exciton dynamics		(NR 8)	(NR 9)	(NR 10)	(NR 11)	Energy level diagram

Fig. 2: Liouville space pathways (LSP) relevant for the calculation of the non-rephasing $\mathbf{K}_{NR} = +2\boldsymbol{K}_1 - 2\boldsymbol{K}_2 + \boldsymbol{K}_3$ signal of molecular dimers and trimers. Single-, bi- and tri-exciton states are labeled by $\{|a_i\rangle\}$, $\{|\alpha_i\rangle\}$ and $\{|f_i\rangle\}$, respectively. The energy level diagram of the considered molecular trimer is depicted at the bottom right. GSB: Ground state bleach, ESA: excited state absorption, SE: stimulated emission.

Molecular dimer:

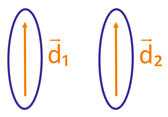

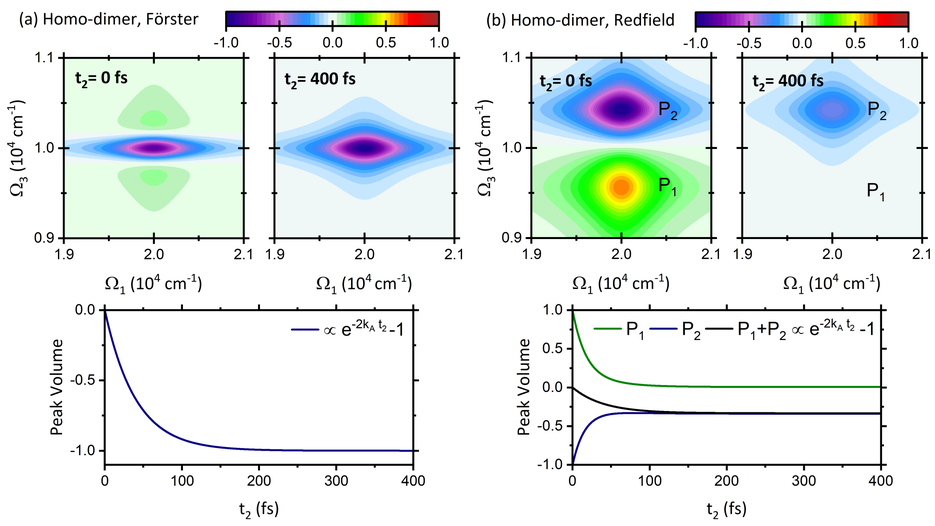

Fig. 5: R^5-2D-ES signal (top panels) of a weakly (a) and strongly (b) coupled homo-dimer for two different waiting times. The bottom panel in both (a) and (b) shows the evolution of the peak volume $V(t_2)$ versus the waiting time t2.
Parameter:
$E = 10^4\ cm^{-1}$, $k_A^{-1} = 80$ fs; Förster: $k_{2->1}^{-1} = k_{1->2}^{-1} = 400$ fs; Redfield: $k_{a2->a1}^{-1} = 17$ fs, $k_{a1->a2}^{-1} = 980$ fs, $J = 420 cm^{-1}$.

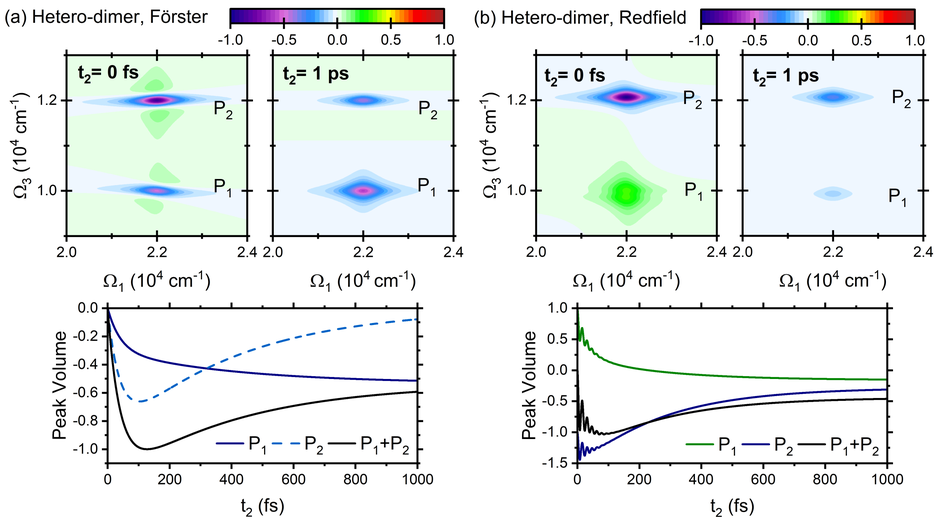

Fig. 6: R^5-2D-ES signal (top panels) of a weakly (a) and strongly (b) coupled hetero-dimer for two different waiting times. The bottom panel in both (a) and (b) shows the evolution of the peak volume versus the waiting time t2.
Parameter:
$E_1 = 10^4\ cm^{-1}$, $E_2 = 1.2 \cdot 10^4\ cm^{-1}$, $d = 2d$, $k_A^{-1} = 80$ fs; Förster: $k_{2->1}^{-1} = 400$ fs, $k_{1->2}^{-1} = 0$ fs; Redfield: $k_{a2->a1}^{-1} = 265$ fs, $k_{a1->a2}^{-1} = 0$ fs, $J = 374\ cm^{-1}$.

$$V(t_2) = 8d_1^2 d_2^2 \Big[\left(d_1^2 + d_2^2\right)\left(G_{\alpha\alpha,\alpha\alpha}(t_2) - G_{gg,gg}(t_2)\right) + \left(d_1^2 - d_2^2\right)\Big(G_{22,22}(t_2) - G_{11,11}(t_2) - G_{11,22}(t_2) + G_{22,11}(t_2) - G_{22,\alpha\alpha}(t_2) + G_{11,\alpha\alpha}(t_2)\Big)\Big]$$

Analytical expression for the peak volume dynamics of a weakly coupled hetero dimer. The signal is directly related to the annihilation rate, in the limit of $d_1^2 = d_2^2$.

Molecular trimer:

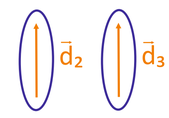

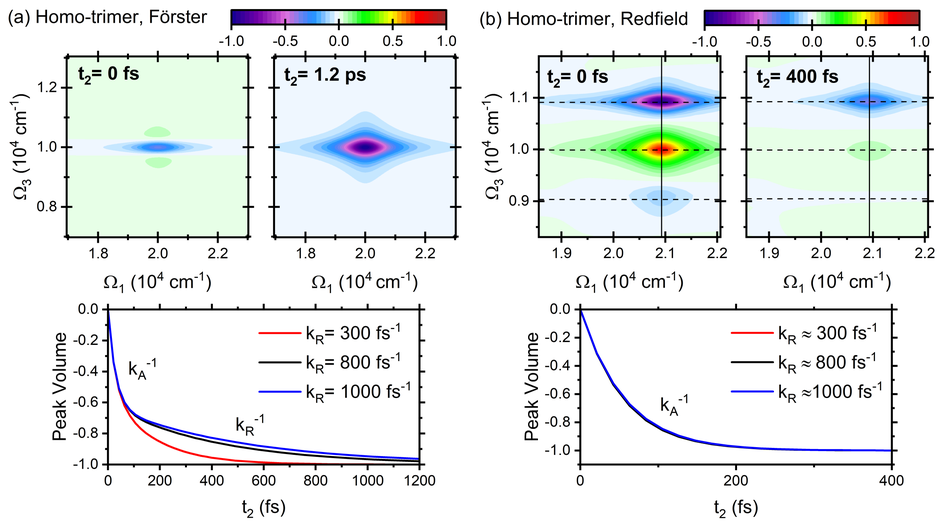

Fig. 7: R^5-2D-ES signal of a weakly (top panels of a) and strongly (top panels of b) coupled homo-trimer for two different waiting times. The bottom panel in both (a) and (b) shows the evolution of the peak volume for different relaxation rates versus the waiting time t2.
Parameter:
$E = 10^4\ cm^{-1}$, $k_A^{-1} = 60$ fs; Förster: $k^{-1} = 300$ fs; Redfield: $k_{a2\ ->\ a1}^{-1} = k_{a3\ ->\ a2}^{-1} = 300$ fs, $k_{a1->a2}^{-1} = k_{a2->a3}^{-1} = k_{a1->a3}^{-1} = 0$ fs, $J_{12} = J_{23} = 630\ cm^{-1}$, $J = 80\ cm^{-1}$.

Conclusion:

- The signal from a homo-dimer is directly related to the annihilation rate.
- The peak volume evolution of the hetero-dimer shows a more involved dependency on both annihilation and transport rates.
- The timescale of exciton diffusion affects the peak volume decay of a weakly coupled trimer, as excitons must migrate to adjacent sites to annihilate. The highly delocalized excitons of a strongly coupled trimer, however, do not allow for more than one stable exciton within the delocalization length and thus no exciton diffusion timescale is visible in the peak volume decay.
- Annihilation dynamics is essential for the appearance of an integrated signal of homo-aggregates of arbitrary length [1].

Objections and suggestions to: Constantin Heshmatpour, c.heshmatpour@tum.de;

References: [1] C. Heshmatpour, et al., Chem. Phys., 110433 (2019), [2] J. Dostál, et al., Nat.Comm. Vol. 9, 2466 (2018), [3] V. May, J. Chem. Phys. 140, 054103 (2014)